



Polymers Hot Paper

 How to cite: *Angew. Chem. Int. Ed.* **2022**, *61*, e202202176

International Edition: doi.org/10.1002/anie.202202176

German Edition: doi.org/10.1002/ange.202202176

Calix[4]pyrrolato Aluminate Catalyzes the Dehydrocoupling of Phenylphosphine Borane to High Molar Weight Polymers

Florian Schön⁺, Lukas M. Sigmund⁺, Friederike Schneider, Deborah Hartmann, Matthew A. Wiebe, Ian Manners,^{*} and Lutz Greb^{*}

Abstract: High molar weight polyphosphinoboranes represent materials with auspicious properties, but their preparation requires transition metal-based catalysts. Here, calix[4]pyrrolato aluminate is shown to induce the dehydropolymerization of phosphine boranes to high molar mass polyphosphinoboranes (up to $M_n = 43\,000$ Da). Combined GPC and ^{31}P DOSY NMR spectroscopic analyses, quantum chemical computations, and stoichiometric reactions disclose a P–H bond activation by the cooperative action of the square-planar aluminate and the electron-rich ligand framework. This first transition metal-free catalyst for P–B dehydrocoupling overcomes the problem of residual *d*-block metal impurities in the resulting polymers that might interfere with the reproducibility of the properties for this emerging class of inorganic materials.

The inclusion of *p*-block elements beyond carbon, nitrogen, and oxygen into polymers paves the way to materials with valuable physicochemical properties.^[1] However, the synthesis of high molar mass polymers with *p*-block element-based main chains remains challenging.^[2] Much effort has been devoted to achieving polycondensation and ring-opening methods to polymerize main-group substrates.^[1,2] Unfortunately, the required substrates are often difficult to prepare. In contrast, dehydrocoupling reactions offer an attractive alternative for the formation of element-element

(E–E) bonds from abundant and convenient precursors, i.e., by the release of H_2 .^[3] Expanding this strategy represents an emerging approach to main-group element polymers and materials.

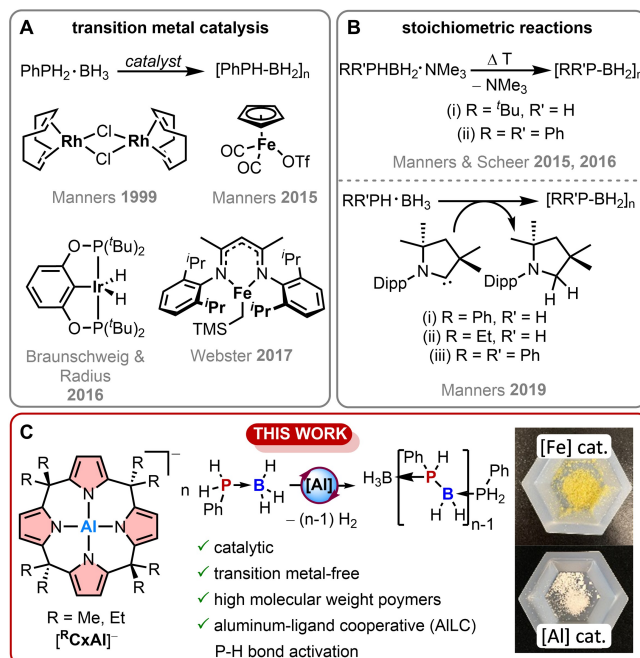
In the 1950s, polyphosphinoboranes sparked interest for the first time due to their high thermal stability and potential use as flame retardants.^[4] However, thermal dehydropolymerization only produced low molar mass, poorly characterizable, and insoluble materials, impeding their use. In 1999, the first approach to high molar mass and soluble polyarylphosphinoboranes was developed using a rhodium-catalyzed dehydropolymerization reaction (Scheme 1A).^[5] Since then, further transition metal-based catalysts containing Ir^[6] or Fe^[7] and a broad field of potential applications were reported (e.g., lithography,^[8] non-linear optics,^[9] or as precursors for boron phosphides^[10]). More recently, the first metal-free routes under mild conditions (22–60 °C) were developed, based on the thermolysis of amine-stabilized phosphinoboranes ($\text{RR}'\text{PBH}_2\cdot\text{NMe}_3$) or by use of cyclic (alkyl)(amino)carbenes (CAACs) as hydrogen acceptors

[*] Dr. F. Schön,⁺ Dr. D. Hartmann, M. A. Wiebe, Prof. I. Manners
 Department of Chemistry, University of Victoria
 Victoria, BC, V8P 5C2 (Canada)
 E-mail: imanners@uvic.ca

L. M. Sigmund,⁺ F. Schneider, Dr. D. Hartmann
 Anorganisch-Chemisches Institut,
 Ruprecht-Karls-Universität Heidelberg
 Im Neuenheimer Feld 270, 69120 Heidelberg (Germany)
 Prof. Dr. L. Greb
 Anorganische Chemie, Freie Universität Berlin
 Fabeckstraße 34–36, 14195 Berlin (Germany)
 E-mail: lutz.greb@fu-berlin.de

[†] These authors contributed equally to this work.

© 2022 The Authors. *Angewandte Chemie International Edition* published by Wiley-VCH GmbH. This is an open access article under the terms of the Creative Commons Attribution Non-Commercial License, which permits use, distribution and reproduction in any medium, provided the original work is properly cited and is not used for commercial purposes.



Scheme 1. Routes for the synthesis of polyphosphinoboranes by A) transition-metal catalysis, B) transition-metal-free stoichiometric reactions, and C) calix[4]pyrrolato aluminate-catalyzed dehydropolymerization described in this work.

(Scheme 1B).^[11] However, multiple-step syntheses of the thermolysis precursors or the need for stoichiometric amounts of CAACs has hindered a large-scale synthesis of the desired polymers.

Another promising strategy is the dehydrocoupling with earth-abundant main-group element-based Lewis acid catalysts. They grant access to a wide range of element-element bonds (e.g. Si–N, Si–Si, or B–N) under mild conditions.^[3b,12] In an early work, the commercially available Lewis acid tris(pentafluorophenyl)borane, B(C₆F₅)₃, enabled the formation of polyphosphinoboranes, but unfortunately only of low molecular weights (up to M_w=3 900 Da).^[13] Consequently, developing transition metal-free catalysts for the dehydrocoupling of phosphine boranes to high molar mass polymers has remained an open challenge.

In recent years, metal–ligand or element–ligand cooperativity (MLC and ELC, respectively) leveraged tremendous progress in bond-activation and catalysis.^[14] Here, both the metal center and its ligand react with a given substrate, offering reaction channels complementary to single-center-based catalysts. In the dehydropolymerization of amine boranes, a series of Fe, Ru, Co, and Rh complexes bearing PNP-pincer ligands were found to operate by metal–ligand cooperative bond activation.^[15] Indeed, high catalytic activity and the high molar mass of the polymers could be traced back to MLC.^[16] Despite these promising results, the MLC concept has never been transferred to the more challenging dehydropolymerization of phosphine boranes.

Herein, we describe the application of calix[4]pyrrolato aluminates,^[17] well-known for metal–ligand cooperativity,^[17b,18] as the first transition metal-free catalysts for the synthesis of high molar mass polyphosphinoboranes (Scheme 1C).

The non-catalyzed polymerization was investigated first. Heating a solution of phenylphosphine borane (**1**) in a mixture of *ortho*-dichlorobenzene (*o*-DCB) and [D₈]toluene (4:1) to 105 °C for 24 h resulted in the slow conversion to polyphenylphosphinoborane, as followed by ¹¹B{¹H} and ³¹P{¹H} NMR spectroscopy. However, GPC analysis revealed the product as a low molar mass material (M_n=2370 Da; Table 1, entry 1) with a high dispersity (Đ) of 4.46.

A prolonged reaction time (48 h) led to a very slight increase in molecular weight (M_n=2770 Da; Table 1, entry 2) but also to an increased dispersity, Đ=7.93. Higher reaction temperatures resulted in undesirable branching processes, as reported earlier,^[5] rendering the non-catalyzed process as an unsuitable source of high molar mass material.

In contrast, the addition of 2.0 mol% of [Li(thf)₄]-[^{Et}CxAl(thf)₂] to a solution of **1** (105 °C, 24 h) resulted in the formation of high molar mass polyphenylphosphinoborane (M_n=17 400 Da; Table 1, entry 4) with Đ=1.84. Increasing the reaction time from 24 h to 48 h produced higher molar mass polymeric material with double the molecular weight (M_n=34 600 Da, Table 1, entry 5), without significantly affecting the dispersity. After a reaction time of 72 h, a molar mass of M_n=39 150 Da was estimated by GPC analysis, accompanied by a decrease in dispersity to 1.66 (Table 1, entry 6). After purification by precipitation, a colorless solid (Scheme 1 C) with M_n=43 010 Da, PDI=1.54 was isolated (Table 1, entry 7, Figures S14–S16). Remarkably, these features are comparable to those of the material obtained with the state-of-the-art transition metal catalysts such as [CpFe(CO)₂][OTf] (M_n=42 000–80 000 Da) under similar conditions.^[7a]

Under the selected reaction conditions, both the background thermal dehydropolymerization and the aluminate-catalyzed reaction should occur. Hence, a critical analysis was needed to obtain mechanistic insight. First, the conversion of **1** with varying amounts of aluminate catalyst was monitored by in situ ¹¹B{¹H} NMR spectroscopy (Figure 1). Increasing the catalyst loading of [Li(thf)₄][^{Et}CxAl(thf)₂] (0.3, 2.0, 5.0, and 10.0 mol%) led to a significant rise of reaction rates, supporting the beneficial catalytic effect of the aluminate under the applied conditions. This was verified quantitatively by NMR spectroscopic determination of pseudo-first-order reaction rate constants (see Supporting Information).

Interestingly, GPC analyses of the isolated polymers revealed a decrease in the molar mass upon increasing the catalyst loading from 2.0 mol% to 5.0 mol% (M_n=15 490 Da, Table 1, entry 8) or 10.0 mol% (M_n=9320 Da, Table 1, entry 9). However, lowering the catalyst loading to

Table 1: Effect of catalysts on the dehydropolymerization of PhPH₂BH₃ (**1**) at 105 °C in a mixture of *o*-DCB/[D₈]toluene (4:1). The conversion was estimated by ¹¹B NMR spectroscopy; nd=not determined. The number and weight average molecular weights (M_n, and M_w, respectively), the dispersity (Đ), and the degree of polymerization (DP) were determined by GPC.

Entry	Catalyst	Catalyst loading mol ⁻¹ %	t [h]	Conversion [%]	M _n [Da]	M _w [Da]	Đ	DP
1	none	–	24	90	2370	10560	4.46	19
2	none	–	48	99	2770	21960	7.93	23
3	[Li(thf) ₄][^{Et} CxAl(thf) ₂]	0.3	24	90	13 580	25 920	1.91	111
4	[Li(thf) ₄][^{Et} CxAl(thf) ₂]	2.0	24	94	17 400	32 080	1.84	143
5	[Li(thf) ₄][^{Et} CxAl(thf) ₂]	2.0	48	99	34 600	62 910	1.82	284
6	[Li(thf) ₄][^{Et} CxAl(thf) ₂]	2.0	72	nd	39 150	64 900	1.66	321
7	[Li(thf) ₄][^{Et} CxAl(thf) ₂] ^[a]	2.0	72	nd	43 010	66 360	1.54	353
8	[Li(thf) ₄][^{Et} CxAl(thf) ₂]	5.0	24	95	15 490	28 310	1.83	127
9	[Li(thf) ₄][^{Et} CxAl(thf) ₂]	10.0	24	100	9320	18 620	2.00	76
10	[PPh ₄][^{Et} CxAl(thf) ₂]	2.0	24	94	19 940	36 540	1.83	164
11	[Li(thf) ₄][^{Me} CxAl(thf)]	2.0	24	94	18 670	36 330	1.95	153

[a] Isolated material.

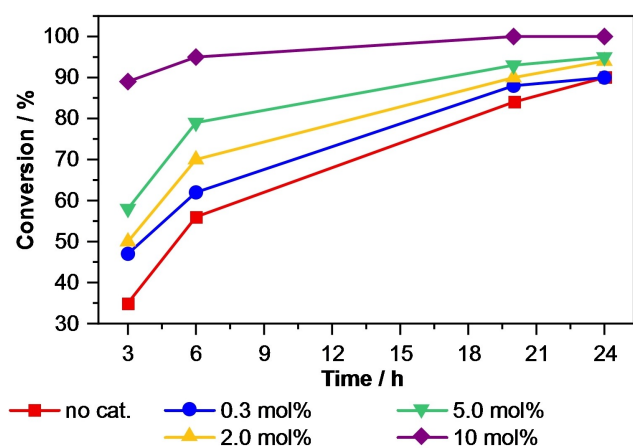


Figure 1. Conversion vs. reaction time plot of the reaction of PhPH_2BH_3 with different catalyst loadings of $[\text{Li}(\text{thf})_4][\text{EtCxAI}(\text{thf})_2]$. The conversion of the substrate (PhPH_2BH_3) was monitored in situ by $^{11}\text{B}\{^1\text{H}\}$ NMR spectroscopy.

0.3 mol% also led to a decrease in molecular weight ($M_n = 13580$ Da, Table 1, entry 3). This suggests that the catalytic process cannot compete with the thermal dehydropolymerization reaction if the catalyst loading is too low.

Substitution of the counterion of the monoanionic aluminate by PPh_4^+ (to eliminate THF from the system) did not significantly alter the composition of the isolated polymeric material (see Supporting Information, Table S2 and Figure S4). This ensures the catalytic relevance of the aluminate, because nucleophiles (such as THF) are known to promote the formation of polyaminoboranes (see below).^[19]

To provide more detailed characterization, samples obtained through preparative GPC separation were studied by $^{31}\text{P}\{^1\text{H}\}$ DOSY NMR experiments. These results were supplemented with DFT-computed ^{31}P NMR chemical shifts. Three different regions in the $^{31}\text{P}\{^1\text{H}\}$ NMR spectra were identified (for details, see Supporting Information): 1) high molar mass polymer (-49 ppm), 2) oligomeric material (-56 to -60 ppm), and 3) branched material (-73 to -90 ppm). The integral ratios of these three regions were 37:49:14 for the uncatalyzed thermal reaction, but 68:29:3 for the aluminate-catalyzed reaction. Hence, these numbers validate the findings from GPC analysis and verify that the aluminate favors the formation of high molar mass linear polymers and minimizes the amount of branched material.

Furthermore, these combined techniques allowed to probe influences of THF or the free ligand, EtCxAI (potentially formed by protonolysis), corroborating the aluminate as the most efficient catalyst (see section 3.10 in the Supporting Information).

To obtain further insight, the reaction of **1** with 2.0 mol% $[\text{Li}(\text{thf})_4][\text{EtCxAI}(\text{thf})_2]$ was analyzed by GPC after different reaction times (Figure 2A). After 1 h (conversion of 21% according to $^{11}\text{B}\{^1\text{H}\}$ NMR spectroscopy), a broad peak at low overall molecular weight ($M_n = 1947$ Da) was observed beside a significant amount of high molar mass material (retention volume of 16.0 mL, $M_p = 29600$ Da).

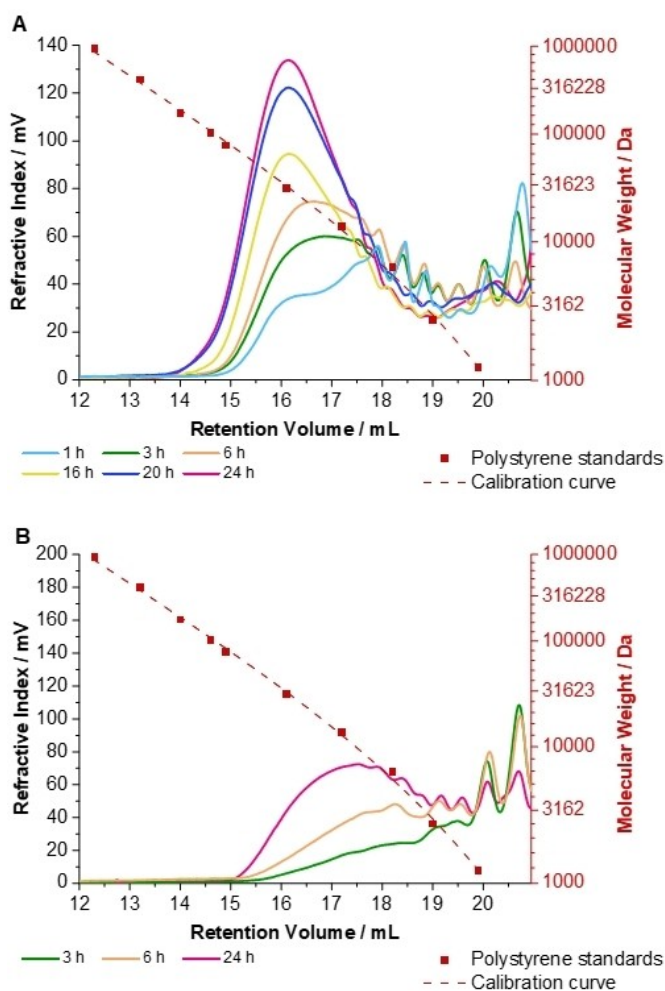


Figure 2. GPC chromatograms (1 mg mL^{-1} in THF with 0.1 wt% $[\text{Bu}_4\text{N}]\text{Br}$ in the THF eluent) of precipitated products obtained after different reaction times A) 2.0 mol% $[\text{Li}(\text{thf})_4][\text{EtCxAI}(\text{thf})_2]$ as catalyst, and B) uncatalyzed reaction.

With prolonged reaction times, the intensity of the latter peak increased continuously. Significantly, the immediate presence of high molar mass material at low conversion suggests the involvement of a chain-growth process. This interpretation is also in line with the decrease in molar mass upon increasing the catalyst loading (Table 1 entries 4, 8, and 9). However, reacting isolated and monomer-free oligomeric material ($M_n = 2600$ Da, obtained from thermal polymerization) with 2.0 mol% of $[\text{Li}(\text{thf})_4][\text{EtCxAI}(\text{thf})_2]$ for 24 h at 105°C led to significant polymer growth to $M_n = 31960$ Da, accompanied with a decrease of the PDI from 6.83 to 1.97. This suggests that the catalyst is able to couple oligomers into higher molar mass polymers, consistent with a step-growth mechanism.^[20] Plotting the molar mass distributions from the GPC versus the conversion did not allow to distinguish between step- or chain-growth polymerization. Notably, the time-resolved GPC measurement for the thermal (non-catalyzed) dehydropolymerization point to a step-growth mechanism, with no distinct high molecular weight peak visible in the GPC trace (Figure 2B). Overall,

the catalytic polymerization appears to be mechanistically complex,^[21] and further experiments are needed to provide conclusive statements.

To obtain insights on the catalyst's mode of action, initial steps were studied by quantum chemical calculations (using $[\text{MeCxAI}]^-$, see Supporting Information for details). Based on some prescreening, deprotonation of the P–H bond in **1** was considered the most viable first reaction. Interestingly, cooperativity of the aluminum center with the 2-position of one of the pyrrole rings was found crucial to facilitate the activation of the P–H bond in **1** both in a kinetic ($\Delta\Delta G^\ddagger = 25 \text{ kJ mol}^{-1}$) and thermodynamic ($\Delta\Delta G_{\text{R}} = 66 \text{ kJ mol}^{-1}$) manner ($\Delta\Delta G$ corresponds to the difference between cooperative and non-cooperative proton transfer, Figure 3A). Hence, $[\text{MeCxAI}]^-$ acts by barrier-lowering via Al-binding-induced acidification of the P–H bond.^[18b] Further calculations suggest this P–H bond activation to enable follow-up H_2 liberation, that is facilitated compared to the monomolecular dehydrogenation of **1** to PhPHBH_2 ($\Delta\Delta G^\ddagger = 14 \text{ kJ mol}^{-1}$, $\Delta\Delta G_{\text{R}} = 63 \text{ kJ mol}^{-1}$, see Supporting Information for mechanistic details).

Indeed, solid experimental evidence for the transfer of a proton from **1** to the 2-position of a pyrrole ring in $[\text{EtCxAI}]^-$ could be obtained. When $[\text{Li}(\text{thf})_4][\text{EtCxAI}(\text{thf})_2]$ was reacted with a substoichiometric amount (0.6 eq) of **1** in $[\text{D}_8]\text{TfHf}$, a selective conversion to $\text{H}\cdot\text{EtCxAI}(\text{thf})_x$, $[\text{PhPH}(\text{BH}_3)_2]^-$, and PhPH_2 occurred (Figure 3B). The formation of $\text{H}\cdot\text{EtCxAI}(\text{thf})_x$ was unambiguously verified by the independent reaction of $[\text{Li}(\text{thf})_4][\text{EtCxAI}(\text{thf})_2]$ with HNTf_2 in $[\text{D}_8]\text{TfHf}$, resulting in identical ^1H NMR resonances (see Supporting Information).

In conclusion, the first transition metal-free catalyst for the dehydropolymerization of phenylphosphine borane is described. Polymers with molar masses up to 43 000 Da were achieved, competing with the current limitations of *d*-block

metal systems. Hence, this method overcomes the problem of residual transition metal-based impurities in the resulting polymer (cf. Scheme 1C), that are potentially detrimental to reproducing the properties in these attractive materials. Stoichiometric reactions and DFT calculations indicate a metal–ligand cooperative P–H bond activation during the reaction cascade, relying on the peculiar electronic structure of the square planar coordinated aluminum anion. These characteristics complement single-center-based transition metal catalysts, enabling alternative modifications for improved performance and selectivity.

Acknowledgements

F.S. acknowledges the Alexander von Humboldt foundation for a Feodor Lynen research fellowship. L.M.S is grateful to the “Studienstiftung des deutschen Volkes” for a scholarship. D.H. is thankful for a fellowship of the Friedrich-Ebert Foundation (FES). M.A.W. is grateful for a NSERC graduate scholarship. I.M. thanks the Government of Canada for a Canada 150 Research Chair and NSERC for a Discovery Grant. L.G. thanks the European Research Council (ERC) under the European Union's Horizon 2020 research and innovation program (grant agreement No. 948708). Markus Enders is acknowledged for NMR measurements and discussions. Open Access funding enabled and organized by Projekt DEAL.

Conflict of Interest

The authors declare no conflict of interest.

Data Availability Statement

The data that support the findings of this study are available in the Supporting Information of this article.

Keywords: Aluminum • Dehydropolymerization • Metal–Ligand Cooperativity • Polymers • Polyphosphinoboranes

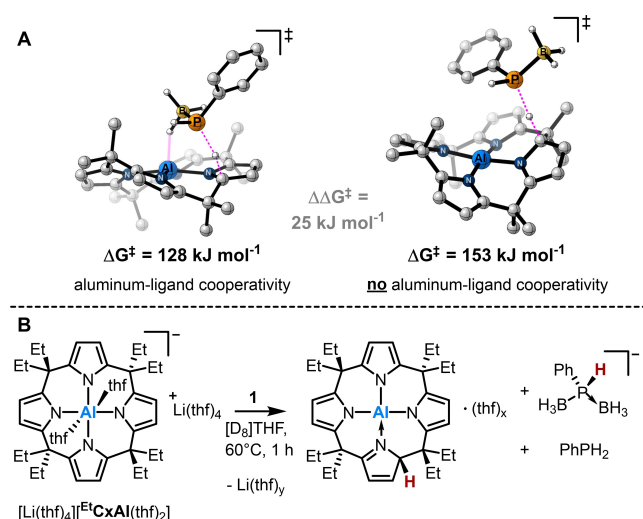


Figure 3. A) Computed aluminum–ligand cooperative P–H bond activation transition state structure (left) and its non-cooperative pendant (right). All C-bound hydrogen atoms were omitted for clarity. B) Reaction of $[\text{Li}(\text{thf})_4][\text{EtCxAI}(\text{thf})_2]$ with substoichiometric amounts (0.6 equiv) of $\text{PhPH}_2 \cdot \text{BH}_3$ (**1**).

- [1] a) I. Manners, *J. Polym. Sci. Part A* **2002**, *40*, 179–191; b) A. L. Colebatch, A. S. Weller, *Chem. Eur. J.* **2019**, *25*, 1379–1390; c) D. Han, F. Anke, M. Trose, T. Beweries, *Coord. Chem. Rev.* **2019**, *380*, 260–286.
- [2] a) A. M. Priegert, B. W. Rawe, S. C. Serin, D. P. Gates, *Chem. Soc. Rev.* **2016**, *45*, 922–953; b) S. Rothmund, I. Teasdale, *Chem. Soc. Rev.* **2016**, *45*, 5200–5215; c) O. Ayhan, N. A. Riensch, C. Glasmacher, H. Helten, *Chem. Eur. J.* **2018**, *24*, 5883–5894; d) F. Vidal, F. Jäkle, *Angew. Chem. Int. Ed.* **2019**, *58*, 5846–5870; *Angew. Chem.* **2019**, *131*, 5904–5929; e) H. R. Allcock, C. Chen, *J. Org. Chem.* **2020**, *85*, 14286–14297.
- [3] a) R. Waterman, *Chem. Soc. Rev.* **2013**, *42*, 5629–5641; b) R. L. Melen, *Chem. Soc. Rev.* **2016**, *45*, 775–788.
- [4] T. Mayer-Gall, D. Knittel, J. S. Gutmann, K. Opwis, *ACS Appl. Mater. Interfaces* **2015**, *7*, 9349–9363.

- [5] H. Dorn, R. A. Singh, J. A. Massey, A. J. Lough, I. Manners, *Angew. Chem. Int. Ed.* **1999**, *38*, 3321–3323; *Angew. Chem.* **1999**, *111*, 3540–3543.
- [6] U. S. D. Paul, H. Braunschweig, U. Radius, *Chem. Commun.* **2016**, *52*, 8573–8576.
- [7] a) A. Schäfer, T. Jurca, J. Turner, J. R. Vance, K. Lee, A. van Du, M. F. Haddow, G. R. Whittell, I. Manners, *Angew. Chem. Int. Ed.* **2015**, *54*, 4836–4841; *Angew. Chem.* **2015**, *127*, 4918–4923; b) N. T. Coles, M. F. Mahon, R. L. Webster, *Organometallics* **2017**, *36*, 2262–2268.
- [8] a) T. J. Clark, J. M. Rodezno, S. B. Clendenning, S. Aouba, P. M. Brodersen, A. J. Lough, H. E. Ruda, I. Manners, *Chem. Eur. J.* **2005**, *11*, 4526–4534; b) J. R. Turner, D. A. Resendiz-Lara, T. Jurca, A. Schäfer, J. R. Vance, L. Beckett, G. R. Whittell, R. A. Musgrave, H. A. Sparkes, I. Manners, *Macromol. Chem. Phys.* **2017**, *218*, 1700120.
- [9] D. Jacquemin, E. A. Perpète, *J. Phys. Chem. A* **2005**, *109*, 6380–6386.
- [10] a) H. Dorn, J. M. Rodezno, B. Brunnhöfer, E. Rivard, J. A. Massey, I. Manners, *Macromolecules* **2003**, *36*, 291–297; b) S. Pandey, P. Lönnecke, E. Hey-Hawkins, *Eur. J. Inorg. Chem.* **2014**, 2456–2465; c) H. Cavaye, F. Clegg, P. J. Gould, M. K. Ladyman, T. Temple, E. Dossi, *Macromolecules* **2017**, *50*, 9239–9248.
- [11] a) C. Marquardt, T. Jurca, K.-C. Schwan, A. Stauber, A. V. Virovets, G. R. Whittell, I. Manners, M. Scheer, *Angew. Chem. Int. Ed.* **2015**, *54*, 13782–13786; *Angew. Chem.* **2015**, *127*, 13986–13991; b) N. L. Oldroyd, S. S. Chitnis, V. T. Annibale, M. I. Arz, H. A. Sparkes, I. Manners, *Nat. Commun.* **2019**, *10*, 1370.
- [12] a) R. J. Less, R. L. Melen, D. S. Wright, *RSC Adv.* **2012**, *2*, 2191–2199; b) L. J. Morris, N. A. Rajabi, M. S. Hill, I. Manners, C. L. McMullin, M. F. Mahon, *Dalton Trans.* **2020**, *49*, 14584–14591; c) L. Wirtz, J. Lambert, B. Morgenstern, A. Schäfer, *Organometallics* **2021**, *40*, 2108–2117.
- [13] J.-M. Denis, H. Forintos, H. Szelke, L. Toupet, T.-N. Pham, P.-J. Madec, A.-C. Gaumont, *Chem. Commun.* **2003**, 54–55.
- [14] a) J. R. Khusnutdinova, D. Milstein, *Angew. Chem. Int. Ed.* **2015**, *54*, 12236–12273; *Angew. Chem.* **2015**, *127*, 12406–12445; b) L. Greb, F. Ebner, Y. Ginzburg, L. M. Sigmund, *Eur. J. Inorg. Chem.* **2020**, 3030–3047.
- [15] a) M. Käß, A. Friedrich, M. Drees, S. Schneider, *Angew. Chem. Int. Ed.* **2009**, *48*, 905–907; *Angew. Chem.* **2009**, *121*, 922–924; b) A. N. Marziale, A. Friedrich, I. Klopsch, M. Drees, V. R. Celinski, J. Schmedt auf der Günne, S. Schneider, *J. Am. Chem. Soc.* **2013**, *135*, 13342–13355; c) A. Glüer, M. Förster, V. R. Celinski, J. Schmedt auf der Günne, M. C. Holthausen, S. Schneider, *ACS Catal.* **2015**, *5*, 7214–7217; d) T. M. Boyd, K. A. Andrea, K. Baston, A. Johnson, D. E. Ryan, A. S. Weller, *Chem. Commun.* **2020**, *56*, 482–485; e) C. N. Brodie, T. M. Boyd, L. Sotorrios, D. E. Ryan, E. Magee, S. Huband, J. S. Town, G. C. Lloyd-Jones, D. M. Haddleton, S. A. Macgregor, A. S. Weller, *J. Am. Chem. Soc.* **2021**, *143*, 21010–21023.
- [16] F. Anke, S. Boye, A. Spannenberg, A. Lederer, D. Heller, T. Beweries, *Chem. Eur. J.* **2020**, *26*, 7889–7899.
- [17] a) F. Ebner, H. Wadeh, L. Greb, *J. Am. Chem. Soc.* **2019**, *141*, 18009–18012; b) F. Ebner, P. Mainik, L. Greb, *Chem. Eur. J.* **2021**, *27*, 5120–5124.
- [18] a) F. Ebner, L. M. Sigmund, L. Greb, *Angew. Chem. Int. Ed.* **2020**, *59*, 17118–17124; *Angew. Chem.* **2020**, *132*, 17266–17272; b) L. M. Sigmund, L. Greb, *Chem. Sci.* **2020**, *11*, 9611–9616; c) L. M. Sigmund, C. Ehlert, M. Enders, J. Graf, G. Gryn'ova, L. Greb, *Angew. Chem. Int. Ed.* **2021**, *60*, 15632–15640; *Angew. Chem.* **2021**, *133*, 15761–15769.
- [19] a) T. Malakar, L. Roy, A. Paul, *Chem. Eur. J.* **2013**, *19*, 5812–5817; b) S. Bhunya, T. Malakar, A. Paul, *Chem. Commun.* **2014**, *50*, 5919–5922; c) A. V. Pomogaeva, A. Y. Timoshkin, *J. Phys. Chem. A* **2021**, *125*, 3415–3424.
- [20] T. Jurca, T. Dellermann, N. E. Stubbs, D. A. Resendiz-Lara, G. R. Whittell, I. Manners, *Chem. Sci.* **2018**, *9*, 3360–3366.
- [21] a) T. N. Hooper, A. S. Weller, N. A. Beattie, S. A. Macgregor, *Chem. Sci.* **2016**, *7*, 2414–2426; b) M. A. Huertos, A. S. Weller, *Chem. Sci.* **2013**, *4*, 1881.

Manuscript received: February 9, 2022

Accepted manuscript online: March 2, 2022

Version of record online: March 29, 2022